

DESIGN AND FREEFORM FABRICATION OF DEPLOYABLE STRUCTURES WITH LATTICE SKINS

Uma Maheshwaraa, Catherine Tradd, David Bourell, and Carolyn Conner Seepersad
Mechanical Engineering Department
The University of Texas at Austin, Austin, TX 78712

Abstract

Frontier environments—such as battlefields, hostile territories, remote locations, or outer space—drive the need for lightweight, deployable structures that can be stored in a compact configuration and deployed quickly and easily in the field. We introduce the concept of lattice skins to enable the design, solid freeform fabrication (SFF), and deployment of customizable structures with nearly arbitrary surface profile and lightweight multi-functionality. Using Duraform FLEX® material in a selective laser sintering machine, large deployable structures are fabricated in a nominal build chamber by either virtually collapsing them into a condensed form or decomposing them into smaller parts. Before fabrication, lattice sub-skins are added strategically beneath the surface of the part. The lattices provide elastic energy for folding and deploying the structure or constrain expansion upon application of internal air pressure. Nearly arbitrary surface profiles are achievable and internal space is preserved for subsequent usage. In this paper, we present the results of a set of experimental and computational models that are designed to provide proof of concept for lattice skins as a deployment mechanism in SFF and to demonstrate the effect of lattice structure on deployed shape.

1. Introduction

Several mechanisms are available for compactly storing and deploying two-dimensional surfaces and three-dimensional structures for applications ranging from the deployment of satellite booms and solar arrays to the construction of temporary shelters and retractable stadium roofs with vast unsupported spans [1,2]. Examples include tensegrity structures comprised of a combination of exclusively compressive and tensile members, as observed in structures such as the Georgia Dome in Atlanta, and pantographs—structural mechanisms with bars connected by pivots at the center point and ends of each bar, and embodied in collapsing laundry racks, temporary gates, and the popular children’s toy, the Hoberman sphere [1,2].

Conventional deployment mechanisms and fabrication techniques generally restrict the geometry of a deployed structure to symmetric, polygonal or spherical shapes and make it difficult to rapidly customize the geometry and functionality of the device. In contrast, a freeform fabrication approach offers several potential advantages, including: (1) the capability of fabricating complex, intricate internal and external geometries, enabling a host of customized, embedded deployment mechanisms and customized parts with nearly arbitrary deployed geometries, (2) rapid design and fabrication cycles, and (3) potentially lightweight, multifunctional structures with embedded mechanisms that not only control deployment but also provide additional functionality such as strength, stiffness, insulation, or blast amelioration. Freeform deployment also has the potential to overcome build chamber size limitations by building large parts in a condensed configuration and deploying them, post-build.

We seek to establish “Design for Freeform Deployment” methods and accompanying solid freeform fabrication (SFF) techniques to enable the design, fabrication, and deployment of customizable structures with nearly arbitrary surface geometry and lightweight multi-functionality. The first step towards this goal is to identify potential deployment mechanisms that are suitable for freeform fabrication and support the desired capabilities. For this purpose, we have devised a particularly promising concept that uses lattice sub-skins for deployment, as illustrated in Figure 1. Beginning with a part of arbitrary surface profile and hollow interior, lattice sub-skins are added beneath the surface of the structure. The part is fabricated using selective laser sintering (SLS) technology and a flexible, elastomer material called Duraflex® FLEX. If the structure is larger than the build chamber, it is decomposed and fabricated as a collection of parts that are subsequently joined together. The flexible structure can be folded for ease of storage and transport and then deployed in the field via a combination of elastic strain energy and pneumatics. In this process, the lattice structure serves several functions. First, during the folding step, it stores strain energy that can be returned upon unfolding to help deploy the structure into its original configuration. Second, in its deployed form, the lattice structure supports the surface of the flexible part to prevent collapse and distortion of desired surfaces. Finally, if elastic energy is insufficient for deploying a large structure under its own weight, air pressure is applied inside the structure, and the lattice skin constrains the expansion of the structure to prevent balloon-like inflation and preserve desired surface profiles. An alternative fabrication route is to collapse the structure virtually (much like deflating a balloon), fabricate it in its condensed form, and then use internal air pressure to inflate the part, with the lattice structure constraining its expansion and preserving the desired surface profile. Fabrication by decomposition is emphasized in this paper.

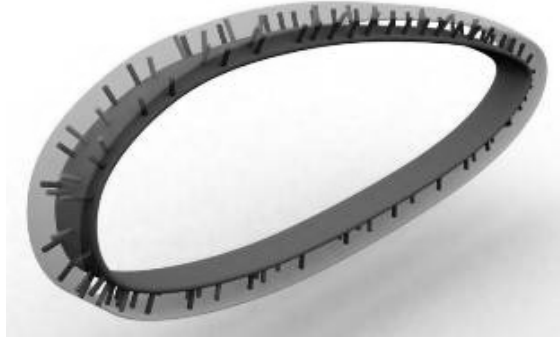


Figure 1. Airfoil section with lattice sub skin

Lattice structures and cellular materials are particularly amenable to solid freeform fabrication techniques, which provide flexibility for fabricating complex, customized lattices or cellular structures as integral aspects of an overall part. Lattice structures and cellular materials have been fabricated with a variety of SFF technologies, including SLS [3], direct metal deposition [4], selective laser melting [5], stereo/photolithography techniques [6,7], and hybrid approaches that include SFF-based sacrificial molds [8,3]. They are used for applications that require lightweight stiffness, compliance, impact absorption, heat exchange, catalysis, and other properties (cf. [9-11] for an overview). However, the use of lattice structures as deployment mechanisms has not been investigated to date.

Lattice structures have several characteristics that make them particularly appropriate for deployment applications. First, they are preferable to internal mechanism-like structures, mentioned previously, because they are more flexible for shape control of relatively arbitrary,

freeform geometries; occupy very little space in the build chamber; and do not require small-scale pivots or joints that are difficult to fabricate. Second, they also offer a combination of low relative density and high effective stiffness, providing high levels of rigidity for controlling the deployment of a three-dimensional part without significantly impacting its apparent density for consolidation and collapse [12]. Third, the lattice skins do not occupy the interior regions of the part, leaving the space available for other uses. In addition, the lattice skin itself makes the deployed part suitable for multifunctional applications [9,11,13,14]. For example, the lattice sub-skin could be filled with cooling fluids or air for heat exchange or insulation; earth, foam, or other materials for impact absorption or blast protection; or explosive materials for controlled detonation. Finally, lattice skins are conducive to portable deployment, requiring only a portable air pump for deployment and a spray can of thermoset coating for rigidization, if desired.

In the following sections, a method is presented for designing, fabricating, and deploying structures with internal lattice sub-skins, and preliminary results are presented.

2. Method for Design and Freeform Fabrication of Deployable Structures with Lattice Sub-skins

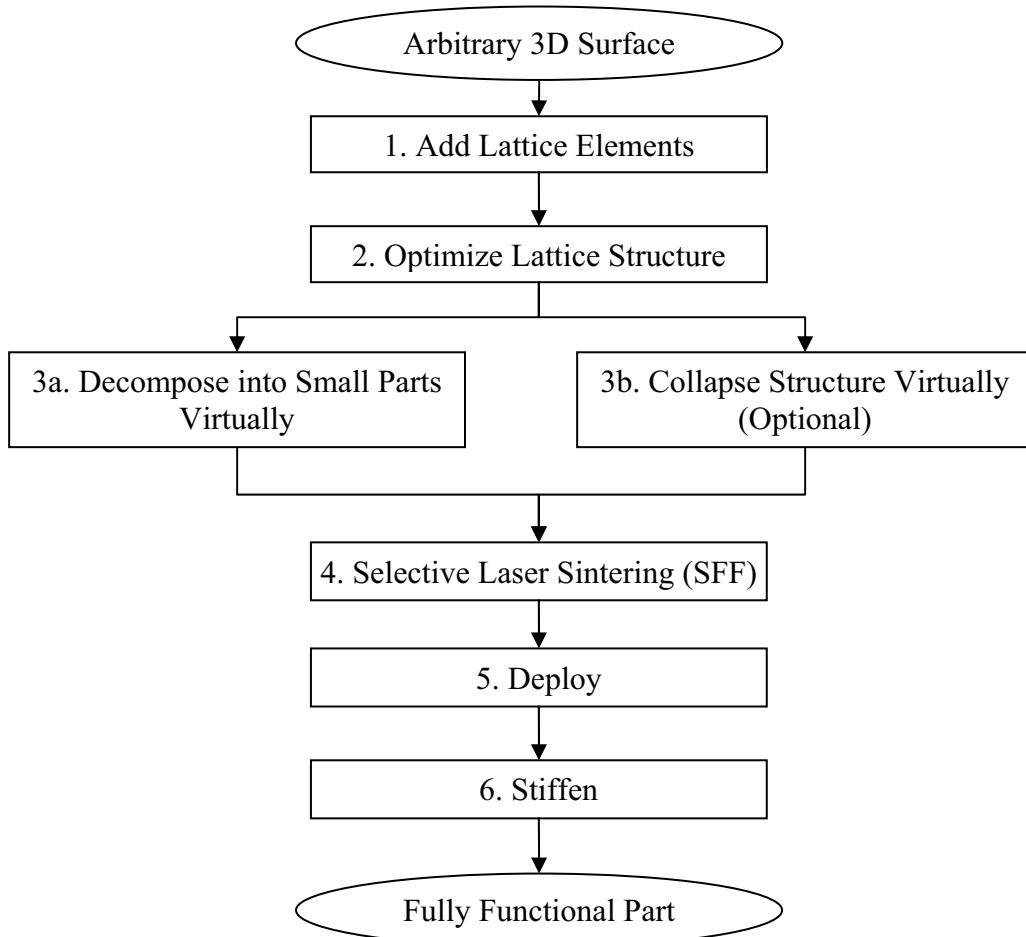


Figure 2. A method for designing and fabricating deployable structures.

The general method for designing and fabricating deployable structures with lattice sub-skins is outlined in Figure 2. The starting point for the method is the 3D surface profile of the part to be deployed. In **Step 1**, a lattice structure is added beneath the surface of the part as a deployment mechanism for deploying the part. The arrangement of the lattice structure could be determined with a topology optimization procedure or a standardized strategy could be applied. An example of a standardized strategy is illustrated in Figure 3, in which the lattice structure is composed of elements oriented perpendicular to the surface of the part and connected with another set of elements that are parallel to the surface of the part. Two types of lattice sub-skins are described in Section 3: (1) an open lattice arrangement, as illustrated in Figure 3, for directly reinforcing the surface of the part, and (2) a closed lattice arrangement for pneumatic inflation.

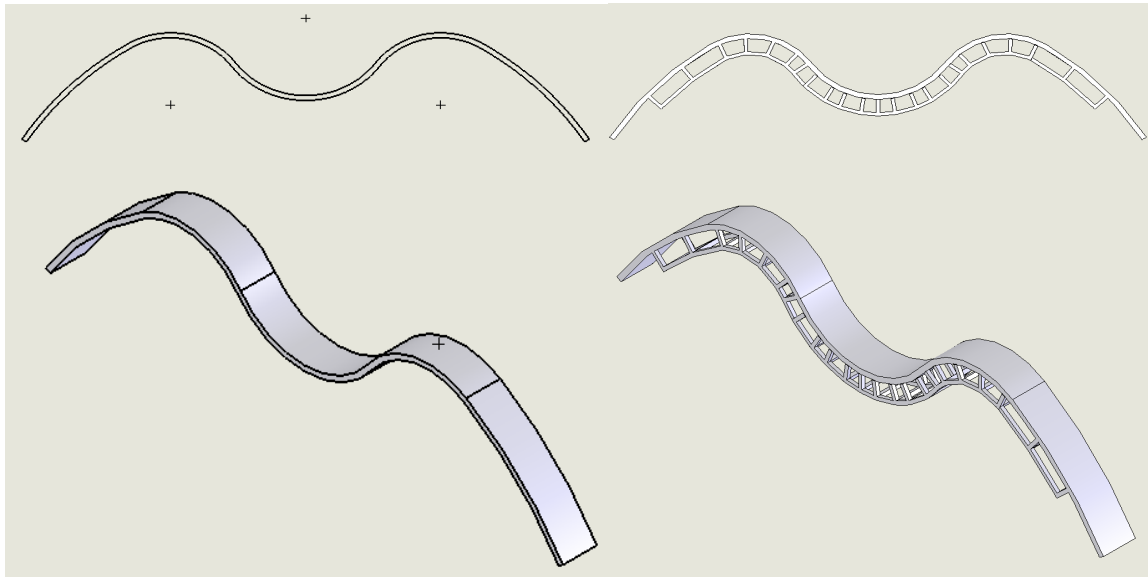


Figure 3. An arbitrary 3D part with added lattice structure.

In **Step 2**, a finite element model of the part and lattice sub-skin is built to analyze the stiffness and deflection profile of the part. If adjustments are needed, the dimensions and density of the lattice structure are varied iteratively until the intended deflection is attained. This step can be executed manually or with an optimization algorithm. For the lattice structure illustrated in Figure 3, the stiffness of the lattice structure should be such that it supports the self-weight of the part with minimal deviation from the intended surface profile. If internal air pressure is used to deploy a closed part, the lattice structure should constrain expansion under internal air pressure so that the intended surface profile is achieved as closely as possible.

The deployment strategy is intended to be applied to large parts with volumes that are greater than that of the SLS build chamber. Therefore, **Step 3** offers two options for overcoming this challenge. As illustrated in Figure 5, the first option is to decompose the structure virtually into parts that are smaller than the build chamber and then assemble and adhere the parts in a post-processing step and fold the flexible structure into a compact, storable package. The second option is to virtually collapse the part in CAD, prototype it in compressed state and expand in a post-processing step to get the final part. This option is similar to wadding or folding a piece of paper and then unfolding it after the build process with a combination of thermal and mechanical

loading. Figure 4 shows a virtually compressed flat plate post-processed to get a part bigger than build chamber.

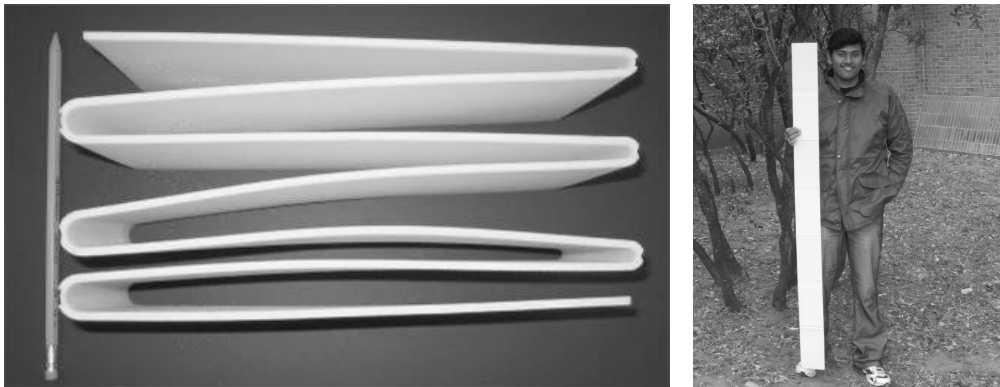


Figure 4. Virtually compressed accordion post processed into a flat plate

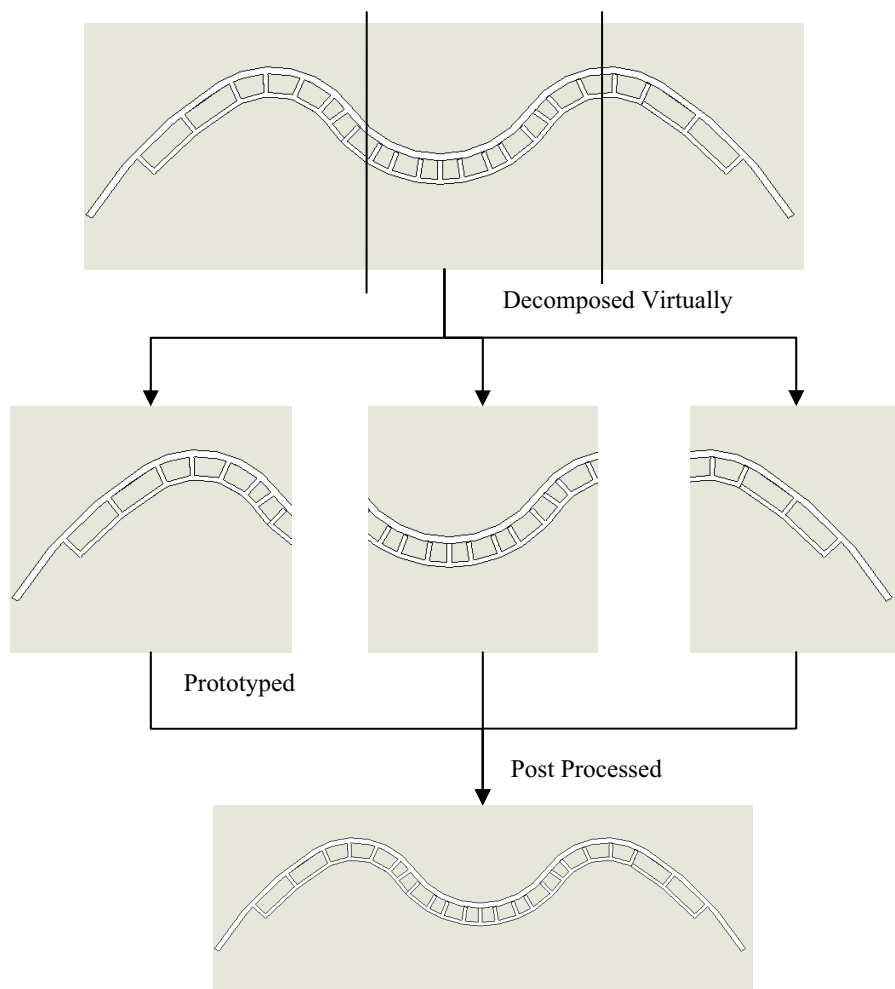


Figure 5. Virtual decomposition of parts larger than the build chamber.

After the part is virtually compressed or decomposed into smaller parts, it is fabricated in the SLS machine using Duraform Flex material in **Step 4**. This step also includes post-processing (e.g., assembling and adhering parts and spraying with an infiltrant to make the parts air-tight).

In **Step 5**, the prototyped part is deployed using internal air pressure and/or any form of mechanical assistance (e.g., human-assisted unfolding). Since the part is constructed of Duraform® FLEX, its skin is quite pliable—a useful feature for folding and storing the part but not for maintaining a rigid structure. If a stiffer skin is desired, the part’s skin can be coated with a thermoset polymer in **Step 6**. The outcome of the method is a fully functional, deployable part.

3. Lattice Structure

An integral part of the methodology for building deployable parts is the deployment mechanism. The lattice structure provides elastic stiffness for supporting the surface of the part and for constraining the expansion of a part during inflation. It can also store elastic strain energy as a large structure is folded and return it as the part is unfolded to aid in the deployment process. Two types of lattice structures are proposed, an open lattice structure (Figure 6a) and a closed lattice structure for air deployable parts (Figure 6b).

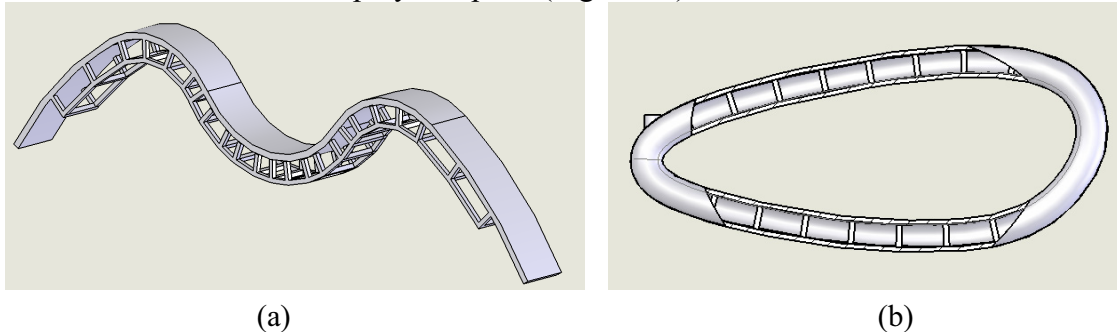


Figure 6. Open lattice (a) for a self-supporting structure and closed lattice (b) for an air deployable part.

3.1 Open Lattice Structure

An open lattice structure is composed of lattice elements added to the inner surface of a part. The arrangement of elements may be determined with a topology optimization routine or by selecting a standard strategy. In the standard strategy illustrated in this paper, lattice elements emanate from the inner surface of a part in an orientation normal to the surface. Their ends are connected by similar lattice elements of same or different dimensions. Rows consisting of numerous lattice elements are added to span the entire surface of the part. Finally the mesh of lattice elements forming the lattice structure is obtained by connecting all the rows. Figure 7 shows the open lattice structure unit for a section of cylindrical surface.

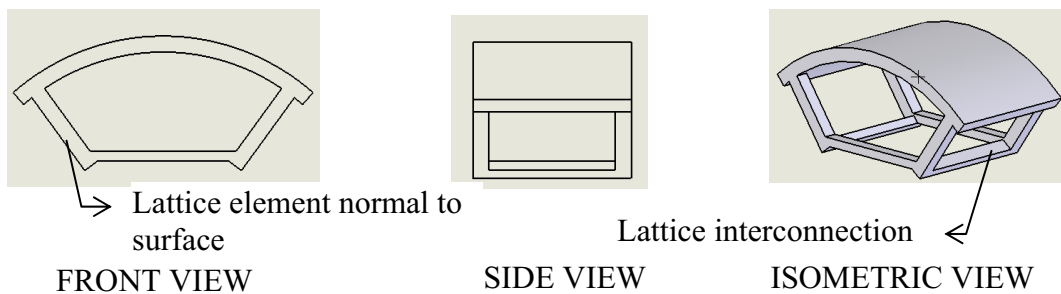


Figure 7. Open lattice unit.

The lattice structure is added to the inner surface in an iterative procedure. The inner surface of a 3D model is used as a reference to create the lattice structure in SolidWorks 2005. In order to maintain the shape of a 3D part, lattice structures are strategically placed beneath the surface to provide support to the surface after deployment. A single lattice element is created normal to the surface at a point. A linear array of the lattice element is added with the curve representing the cross section as a guide. This is then extended along the depth of the curve to generate lattices over the entire inner surface. The spacing of the elements in all directions is decided based on the lattice density required for the part.

The dimensions and density of the lattice structure play a vital role in making the deployable part. The lattice element density beneath the surface depends not only on the geometry of the surface and the target deflection profile but also on the stiffness of the Duraform® FLEX material. The laser power of the SLS machine can be adjusted to alter the stiffness of the Duraform® FLEX material. If the material is highly flexible, the lattice elements are more densely spaced and/or larger in dimension to provide more support to the flexible surface.

Finite element analysis (ANSYS [15]) is used to determine the appropriate density and dimensions of the lattice structure for maintaining the surface profile of the final part. The procedure is iterative. The initial dimension of the lattice element is set to 2 mm x 2 mm because the resolution of the SLS machine can be poor for smaller elements. Depending upon the surface deflection estimates, the lattice element sizes and densities are iteratively adjusted until the deflections are acceptable. Eventually, the iterative procedure will be guided by an optimization method that may provide better results faster. Figure 8 shows the iterative procedure to generate lattice structure for any part. The ANSYS models are described in Section 4.

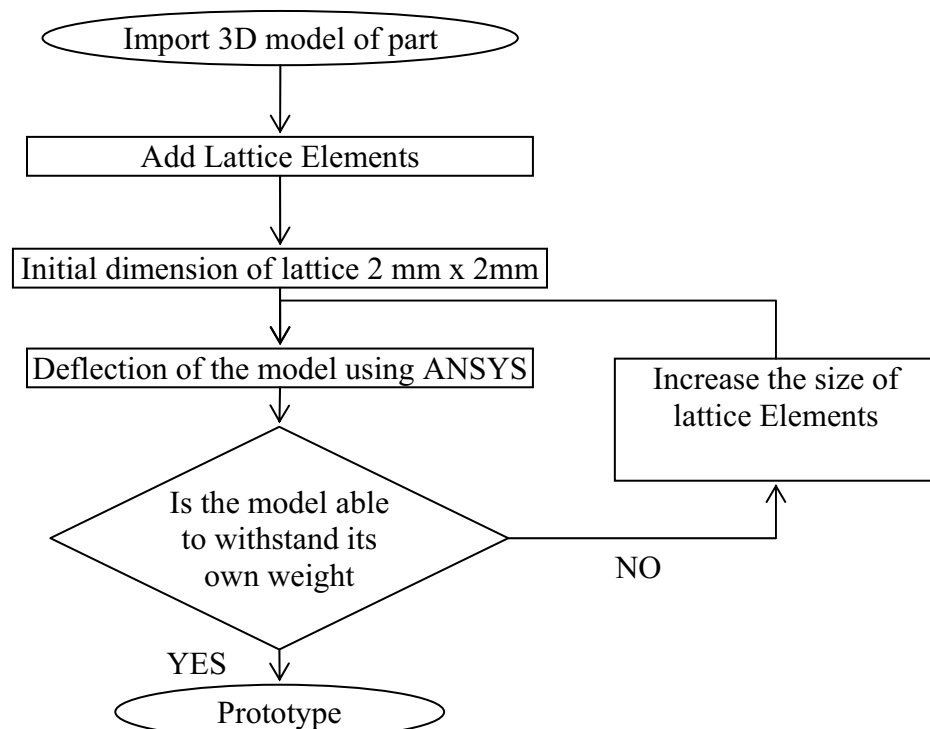


Figure 8. Methodology for generating lattice structure.

3.2 Closed Lattice Structure for Pneumatic Deployment

If air pressure is used to deploy the structure, a closed lattice structure is created to join the outer surface of the part with a concentric, inner surface that is separated from the outer surface everywhere by a set distance, as illustrated in Figure 9. For deployment, pressurized air is pumped between the concentric skins. Lattice structures join the surfaces at strategic points, and they are oriented to be perpendicular to both skins. The lattice structure mainly helps in maintaining the shape when air is pumped in between the parallel surfaces. Without the lattice structure, the skin would expand naturally to a sphere-like shape, with maximum ratio of volume to surface area. The lattice skin constrains the expansion so that the volume between the two surfaces is maximized, which occurs when the skins are concentric and the lattice elements are stretched to maximum length. Figure 9 shows a section of an air foil with lattice structure connecting inner and outer surface.

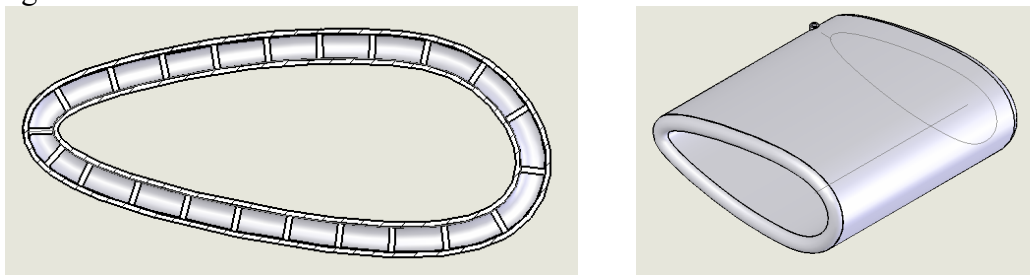


Figure 9. Deployable structure with air as the deployment mechanism.

The final part will have non-uniform densities of lattice elements, with the arrangement depending on curvature and desired surface accuracy. Broader spacing essentially provides less stiffness between the skins, allowing the outer skin to expand more when air is pumped into the part. Broader spacing can yield bulges in the surface of the part between lattice elements, similar to the bulges in a riveted pillow. If the accuracy requirements or curvature rate is higher in a particular section, the lattice elements in that section are more densely arranged to provide tighter control over the surface profile during deployment.

4. Proof of Concept with Virtual and Physical Prototypes

To evaluate the feasibility and effectiveness of the proposed deployment strategy, we developed finite element models of sample deployable structures in ANSYS and created corresponding prototypes with SLS and Duraform® FLEX material.

4.1 Finite Element Modeling in ANSYS

Finite element analysis of Duraform® FLEX parts needs to account for the elastomeric behavior of the material with its relatively large Poisson's ratio and large displacements under relatively small applied loads. To model the behavior of a part composed of Duraform® FLEX that undergoes large deformations, we developed finite element analysis models in ANSYS and utilized its geometrically nonlinear analysis capabilities. Before analyzing deployable structures, we calibrated our models with some simple experimental tests. A cantilever beam test was done on a Duraform® FLEX block of dimensions 93.5 mm x 32.5 mm x 3.5 mm. As shown in Figure 10, the boundary conditions included fixed deflection and rotation at one end of the specimen

and a set of increasing loads applied to the opposite end. Data for deflection as a function of applied load are recorded in Table 1. Material properties of the specimens were also evaluated and listed in Table 2. These material properties vary according to SLS build parameters such as laser power [16][17]. Accordingly, the properties were evaluated from the set of test parts, and the same build parameters were used for prototyping.

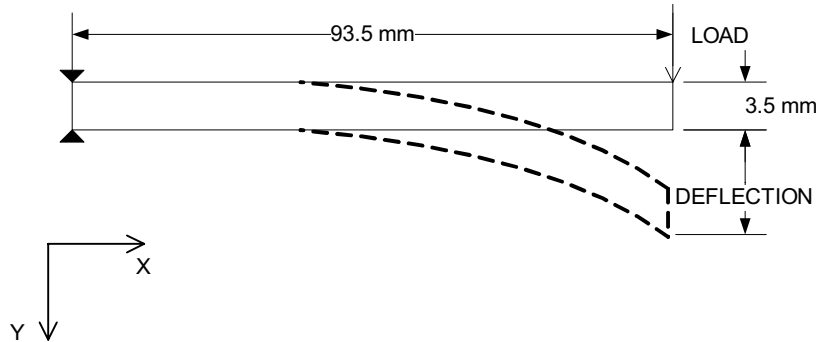


Figure 10. Schematic diagram for cantilever beam test.

Table 1. Displacement in y-direction.

Load (N)	DEFLECTION (mm)
0.16785	24.61
0.355231	30.22
0.462616	30.98
0.576859	35.12
0.852239	37.08

Table 2. Material properties for ANSYS analysis.

Property	Value
EX (Tensile Modulus)	3.8 MPa
Density	486.1 kg/m ³
Poisson Ratio	0.45

A corresponding three-dimensional finite element model of the specimen was developed in ANSYS, using the appropriate material properties. Both large deformation and small displacement analyses were conducted, and the results were compared with experimental data in Figure 11. For both analyses, a SOLID45 element was used with element size of 0.15 mm (measured by edge length). In a small displacement analysis, the load is applied in a single step, and it is assumed that the geometry of the part is unchanged—an assumption that leads to very little error if the deformation is small. When the large deformation analysis is enabled in ANSYS, the load is applied incrementally in a series of steps. After each step, ANSYS updates the geometry to reflect the simulated deformations. The number of load steps for the large deformation analysis was set to 200.

As shown in Figure 11, the large deformation model matches the experimental data much more closely than the small displacement model over a broader range of displacements. The small displacement model is very accurate for small displacements, but increasingly overestimates deflection as the magnitude increases. As shown in Figure 11, the force-deflection curve for the small displacement model is linear, as opposed to the nonlinear relationship observed experimentally. The large deformation model is relatively accurate over the entire range of displacements and typically approximates the experimentally measured deflection

within 10%. With the low magnitude of Duraform® FLEX's elastic modulus, large deflections are expected and may even occur under self-weight for large structures.

The simple experiment confirms our capability of analyzing the force-deflection behavior of simple structures composed of Duraform® FLEX material, using large deformation analysis in ANSYS. The next step is to demonstrate how we can use this capability to analyze and design fully deployable structures.

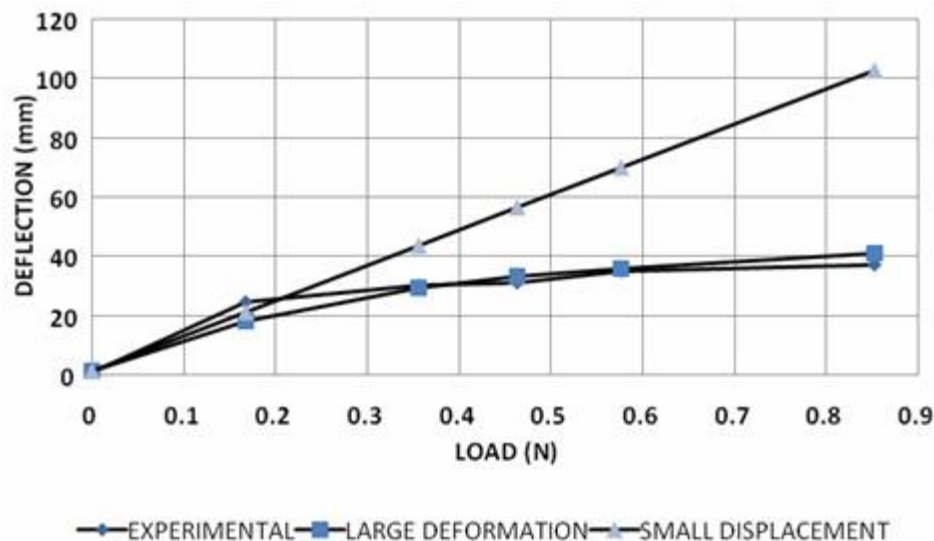


Figure 11. Comparison of deflection values between experiments and ANSYS.

4.2 Physical Prototypes

Two different arch prototypes were used to study the ability of lattice structure to maintain the required profile. The first prototype—illustrated in Figure 12 and Figure 13—is a single arch with overall dimensions of 30 cm (length) x 8 cm (height) x 0.3 cm (thickness of skin). Prototypes of the arch were fabricated with and without the underlying lattice structure, with identical dimensions for the length, height, and thickness of the outer skin. Both prototypes were fabricated in an identical arched shape. As shown in Figure 12, the arch collapses under its own weight without the underlying lattice structure. The center of the lattice prototype deflects vertically by 2.1 cm under its own weight. As shown in Figure 13, ANSYS models of the structure predict a deflection of 2.0 cm, within 5% of the actual experimental value. In the ANSYS model, the effect of self weight was simulated by adding gravitational body forces and specifying the measured density of the Duraform® FLEX material. Boundary conditions included constraints on horizontal and vertical deflection on one end of the arch and constraints on vertical deflection on the other end.

The second prototype—illustrated in Figure 14-Figure 17—is a double arch with overall dimensions of 30 cm (length) x 7 cm (height) x 0.3 cm (thickness of skin). The purpose of constructing a second prototype was to investigate a more arbitrary surface profile with convexities and concavities in the surface. As illustrated in the figures, prototypes of the double arch were also fabricated with and without the lattice structure, with all other features identical.

As shown in Figure 14 and Figure 17, the prototype without the lattice structure collapsed under its own weight to a single, concave arch. As shown in Figure 15 and Figure 16, the prototype with the lattice structure retained its shape. The center of the prototype deflects vertically by 1.1 cm under its own weight. ANSYS models of the structure predict a deflection of 1.1 cm, within 1 % of the actual experimental value. Boundary conditions were identical to those of the single arch model.

A larger prototype of the single arch was also created with dimensions of 90 cm (length) x 30 cm (height) x 0.9 cm (thickness of skin). The deflection in the centre of the prototype was measured to be 19.8 cm due to its own weight. ANSYS models of the prototype predict a deflection of 18.7 cm, within 5% of the actual experimental value. The boundary conditions were identical to the previous models.



Figure 12. Arch prototype with and without lattice structure.

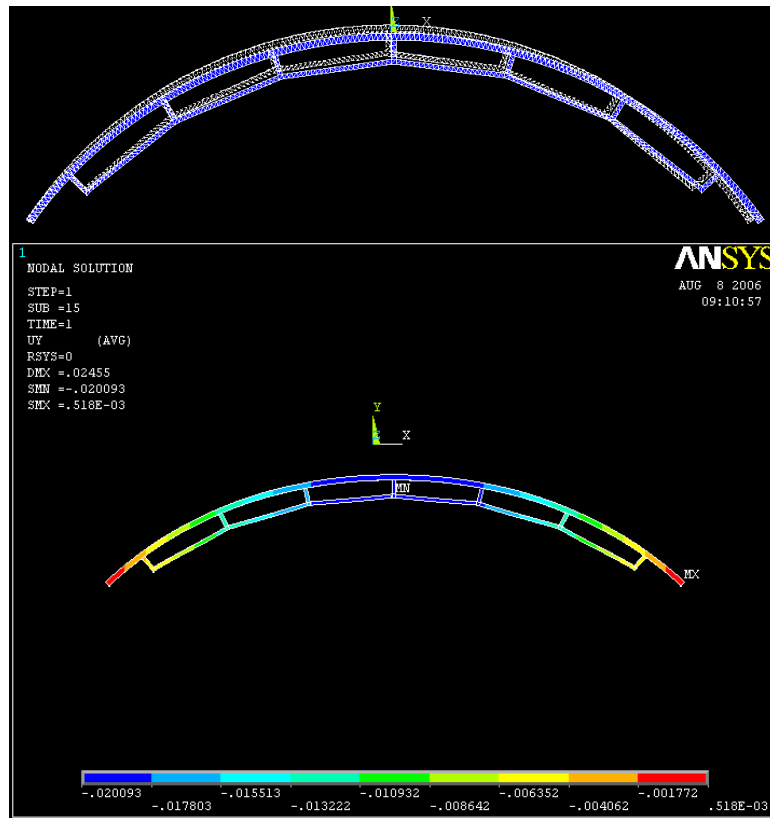


Figure 13. ANSYS model of the arch withstanding its own weight. Colors represent displacement contours with blue contours on the order of 2 cm for an arch with a span of 30 cm and height of 8 cm.

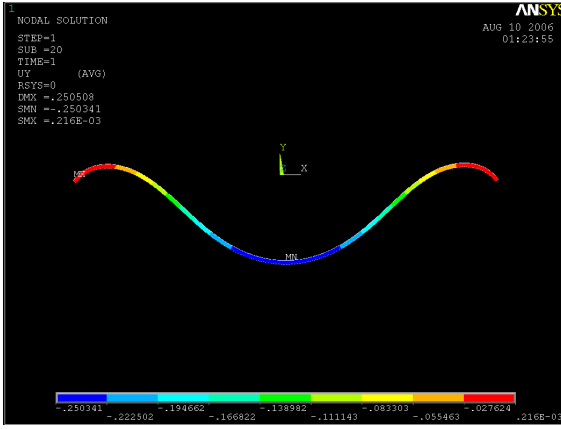


Figure 14. ANSYS result for the double arch without lattice structure, showing deflection contours under self weight. Blue contours represent maximum deflection, on the order of 25.03 cm, which occurs where the convex arches collapse.

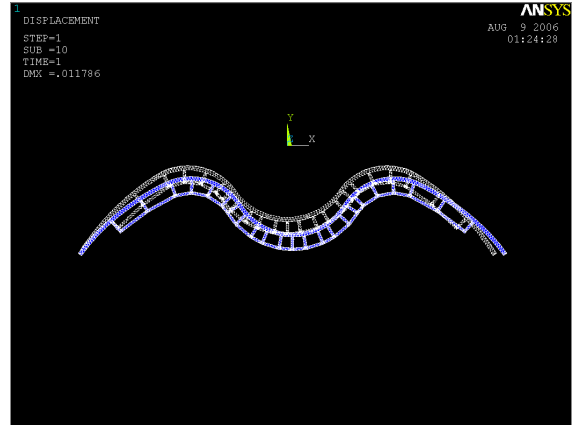


Figure 15. ANSYS result showing the double arch with lattice structure maintaining its profile. Dotted lines represent the original, undeformed shape.

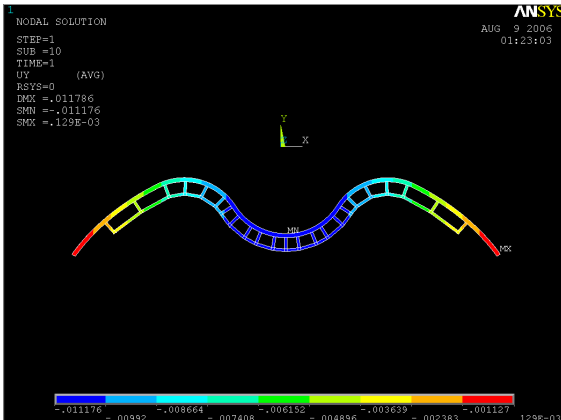


Figure 16. ANSYS result of the double arch with lattice structure showing the deflection contours. Blue contours represent maximum vertical deflection, on the order of 1.1 cm.

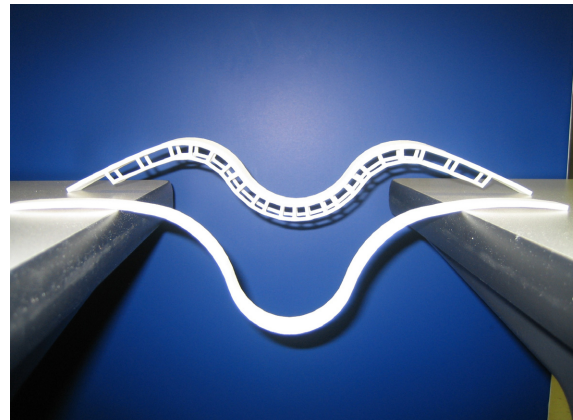


Figure 17. 3D Concave arch with and without the lattice structure

5. Closure

A method has been presented for designing and fabricating deployable structures, with lattice structures as the deployment mechanism. The deployable structures are fabricated from an elastomeric Duraform® FLEX material using selective laser sintering (SLS). The flexible, elastomeric material allows the structures to be folded and compactly stored. For achieving a target surface profile during deployment, lattice structures are utilized both to reinforce the surfaces of flexible structures when they are unfolded and to constrain their expansion when they are pneumatically deployed. Virtual and physical prototypes provide proof of concept for some preliminary designs with open lattice structures for reinforcement of both convex and concave surface profiles. Future work involves virtual and physical prototyping of deployable structures with closed lattice structures and pneumatic deployment. Prototyping the closed lattice

deployable structures involves several challenges, such as sealing the part with a polyurethane infiltrant to withstand air pressure during deployment and spray coating with a thermoset polymer for stiffness after deployment. Also, an important aspect of the deployment methodology involves prototyping parts that are larger than the SLS build chamber. Currently, large structures are decomposed into smaller parts for fabrication in a nominal build chamber. Future work involves developing strategies for virtually collapsing (folding, rolling, wadding) the parts in CAD and post-processing the parts to return them to their intended configurations.

6. Acknowledgments

We gratefully acknowledge financial support from the University of Texas at Austin. We owe a special thanks to the undergraduate students who participated in this project: Brian Nowotny, Trevor Page, and Brandon Walther.

7. References

1. Gantes, C. J., 2001, *Deployable Structures: Analysis and Design*, WIT Press, Boston.
2. Pellegrino, S., Ed., 2001, *Deployable Structures*, International Center for Mechanical Sciences, CISM Courses and Lectures No. 412, Springer-Verlag, New York.
3. Stampfl, J., H. Fouad, S. Seidler, R. Liska, F. Schwager, A. Woesz and P. Fratzl, 2004, "Fabrication and Moulding of Cellular Materials by Rapid Prototyping," *International Journal of Materials and Product Technology*, Vol. 21, No. 4, pp. 285-296.
4. Oruganti, R. K., A. K. Ghosh and J. Mazumder, 2004, "Thermal Expansion Behavior in Fabricated Cellular Structures," *Materials Science and Engineering A*, Vol. 371, pp. 24-34.
5. Brooks, W., C. Sutcliffe, W. Cantwell, P. Fox, J. Todd and R. Mines, 2005, "Rapid Design and Manufacture of Ultralight Cellular Materials," *Proceedings of the Solid Freeform Fabrication Symposium* (D. L. Bourell, R. H. Crawford, J. J. Beaman, K. L. Wood and H. L. Marcus, Eds.), Austin, TX.
6. Zimbeck, W. R. and R. W. Rice, 1999, "Freeform Fabrication of Components with Designed Cellular Structure," *Solid Freeform and Additive Fabrication, Materials Research Society Symposium Proceedings* (D. Dimos, S. C. Danforth and M. J. Cima, Eds.), Materials Research Society, Warrendale, PA, Vol. 542.
7. Wang, H., 2005, "A Unit Cell Approach for Lightweight Structure and Compliant Mechanism," *Ph.D. Dissertation*, G.W. Woodruff School of Mechanical Engineering, Georgia Institute of Technology, Atlanta, GA.
8. Gervasi, V. R. and D. C. Stahl, 2004, "Design and Fabrication of Components with Optimized Lattice Microstructures," *Proceedings of the Solid Freeform Fabrication Symposium* (D. L. Bourell, R. H. Crawford, J. J. Beaman, K. L. Wood and H. L. Marcus, Eds.), Austin, TX.
9. Gibson, L. J. and M. F. Ashby, 1997, *Cellular Solids: Structure and Properties*, Cambridge University Press, Cambridge, UK.
10. Evans, A. G., J. W. Hutchinson and M. F. Ashby, 1999, "Multifunctionality of Cellular Metal Systems," *Progress in Materials Science*, Vol. 43, No. 3, pp. 171-221.

11. Evans, A. G., J. W. Hutchinson, N. A. Fleck, M. F. Ashby and H. N. G. Wadley, 2001, "The Topological Design of Multifunctional Cellular Materials," *Progress in Materials Science*, Vol. 46, No. 3-4, pp. 309-327.
12. Hayes, A. M., A. Wang, B. M. Dempsey and D. L. McDowell, 2004, "Mechanics of Linear Cellular Alloys," *Mechanics of Materials*, Vol. 36, No. 8, pp. 691-713.
13. Seepersad, C. C., B. M. Dempsey, J. K. Allen, F. Mistree and D. L. McDowell, 2004, "Design of Multifunctional Honeycomb Materials," *AIAA Journal*, Vol. 42, No. 5, pp. 1025-1033.
14. Seepersad, C. C., R. S. Kumar, J. K. Allen, F. Mistree and D. L. McDowell, 2005, "Multifunctional Design of Prismatic Cellular Materials," *Journal of Computer-Aided Materials Design*, Vol. 11, No. 2-3, pp. 163-181.
15. ANSYS, Version 10.0, 2006.
16. Levy, G. N., P. Boehler, R. Martinoni, R. Schindel and P. Schleiss, 2005, "Controlled Local Properties in the Same Part with Sintaflex--A New Elastomer Powder Material for the SLS Process," *Solid Freeform Fabrication Symposium* (D. L. Bourell, R. H. Crawford, J. J. Beaman, K. L. Wood and H. L. Marcus, Eds.), Austin, TX.
17. http://www.3dsystems.com/products/datafiles/lasersintering/datasheets/DS-DuraForm_Flex_plastic.pdf.